

# Effects of strong magnetic fields on the population of hyperon stars

R.O. Gomes<sup>1,2,\*</sup>, V. Dexheimer<sup>3</sup>, and C.A.Z. Vasconcellos<sup>1,4</sup>

<sup>1</sup> Instituto de Física, Universidade Federal do Rio Grande do Sul, Av. Bento Gonçalves 9500, CEP 91501-970, Porto Alegre, RS, Brazil

<sup>2</sup> Frankfurt Institute for Advances Studies, Ruth-Moufang-Strasse 1 60438 Frankfurt am Main

<sup>3</sup> Department of Physics, Kent State University, Kent OH, 44242 USA

<sup>4</sup> ICRANet, P.zza della Repubblica 10, 65122 Pescara, Italy

Received 2014 Apr 30, accepted 2014 May 30

Published online 2014 Aug 01

**Key words** equation of state - elementary particles - magnetic fields - stars: neutron

In this contribution we study the effects of strong magnetic fields on the particle population of neutron stars with hyperon degrees of freedom in their composition. The star matter is described by a multi-component model with parameterized baryon-meson interaction couplings. We study the magnetic effects on the equation of state (EoS) due to the Landau quantization, assuming a density dependent static magnetic field that reaches about  $10^{19}$  G in the center of the star. The Tolman-Oppenheimer-Volkoff equations are solved in order to understand the dependence of the mass-radius relation and hyperon population on the magnetic field intensity assuming different interaction coupling schemes.

© 2014 WILEY-VCH Verlag GmbH & Co. KGaA, Weinheim

## 1 Introduction

In recent years, magnetars have attracted increasing attention due to their extremely powerful magnetic fields and the emission of high-energy electromagnetic radiation, particularly X-rays and gamma rays, broadening our conceptions about the formation and evolution of neutron stars. Magnetars are neutron stars with strong magnetic fields, whose intensities are larger than the critical value at which the energy between Landau quantized levels of electrons equals their rest mass.

The critical value for the intensity of the magnetic field in neutron stars can be estimated by assuming that electronic Landau levels, i.e., the discrete energy values  $E_n$  of the orbits of electrons under the action of an external magnetic field  $B$ , may be described by the quantum states of the three dimensional harmonic oscillator  $E_n = \hbar\omega \left(n + \frac{3}{2}\right)$ , with  $n = 0, 1, 2, 3, \dots$ . From this expression, we obtain the separation  $\Delta E_{n,n+1}$  between successive Landau levels, labelled respectively as  $n$  and  $n + 1$ :

$$\Delta E_{n,n+1} = \hbar\omega. \quad (1)$$

Taking the classical cyclotron frequency  $\omega$  of the orbital motion of an electron in a magnetic field  $\omega = \frac{eB}{m_e c}$ , we obtain  $B = m_e c \frac{\omega}{e}$ , where  $m_e$  represents the electron mass and  $e$  its electrical charge, and assuming  $\Delta E_{n,n+1} = \hbar\omega = m_e c^2$  allows one to estimate the critical value  $B_C$  of the magnetic field

$$B_C = \frac{m_e^2 c^3}{\hbar e} \sim 4.4 \times 10^{13} \text{ G}. \quad (2)$$

\* Corresponding author: e-mail: rosana.gomes@ufrgs.br

Compact objects with surface magnetic fields as strong as  $10^{14} - 10^{15}$  G, have been observed and this has drawn the attention to the study of the equation of state (EoS) of hadronic matter in the presence of strong magnetic fields. The intensity of magnetic fields in the interior region of magnetars are expected to be even stronger, maybe reaching  $10^{19}$  G (Ferrer et al 2010).

According to Rea & Esposito (2011), the large magnetic field of a magnetar causes extreme activity such as large outbursts (during which their X-ray flux output can increase by several orders of magnitude) accompanied by short energetic X-ray bursts. However, there is some controversy about the origin of such intense magnetic fields inside neutron stars. Candidates for magnetars are often referred as Soft Gamma Repeaters (SGRs) or Anomalous X-Ray Pulsars (AXPs), depending on the characteristics of their electromagnetic emissions. For a review of this topic see Woods & Thompson (2006) and Mereghetti (2008). There are however alternative models to the magnetar scenario, for instance the white dwarf model which describes the SGRs and AXPs powered by the rotational energy of a massive, fast rotating, highly magnetized white dwarf with surface fields in the range  $10^8 - 10^{10}$  G (see Malheiro et al 2012, for details).

Strong magnetic fields may also be very important for neutron star formation. Stars more massive than about 8 solar masses and less massive than about 25 solar masses in the beginning of their lives are supposed to be the prime candidates for the standard formation scenario behind core-collapse supernovae. During this process, when the star core reaches nuclear densities, nuclear forces and the neutron de-

generacy pressure sharply increase the core internal pressure, causing the core to bounce sending a shock wave throughout the star (Bethe & Brown 1998). The nature of the bounce mechanism depends upon the equation of state of the core: accordingly, a stiffer equation of state causes the star to bounce more quickly but also more weakly than a softer equation of state. As an alternative scenario, magnetic fields may deposit enough energy on the proton-neutron star and drive the explosion. Within the current uncertainties in these mechanisms, strong magnetic fields produce massive neutron stars, in agreement with the astronomical observations.

Finally, the presence of stable matter at super-nuclear densities in neutron stars makes then essential tools for the understanding of hadronic physics. An important feature in neutron stars is the possibility of new hadronic degrees of freedom, in addition to neutrons and protons. Hyperons, i.e., baryons with strange content, are hypothesized to appear in the dense interior of neutron stars at about twice the nuclear saturation density. This can easily be explained by the Pauli principle, since as the baryon density increases, the same occurs with the Fermi momentum and the Fermi energy, thereby enlarging the phase space of the baryon sector. Note that the predominant effect of the presence of hyperons is to soften the equation of state of nuclear matter, due to the decay of energetic nucleons at the top of the Fermi sea into hyperons at lower Fermi levels, generating as a consequence neutron stars with smaller masses. Nevertheless, is not a sufficient argument to ignore the hyperons, as discussed in detail in Ref. (Buballa et al. 2014).

In this work, we study the combination of the two aforementioned ingredients in order to understand the hyperon role in the composition of stellar matter and the respective mass-radius relationship, and compare our predictions with a recent observation that accounts for a neutron star mass of the order of two solar masses (Demorest, P. et al, 2010). We examine the role of the presence of hyperons in the core of neutron stars with emphasis on effects that can be attributed to the general multi-species composition of nuclear matter. With this goal, we study the effects of intense magnetic fields on the population and also in global properties of neutron stars, using a relativistic effective model with parameterized couplings involving the interaction between nucleons, hyperons and mesons.

## 2 Model description

We consider in this paper a scalar version of the effective relativistic QHD-model with parameterized couplings. This model represents an extended compilation of other QHD models found in the literature (Vasconcellos 2012). The complete expression of our scalar QHD interaction Lagrangian exhausts the whole fundamental baryon octet ( $n$ ,  $p$ ,  $\Sigma^-$ ,  $\Sigma^0$ ,  $\Sigma^+$ ,  $\Lambda$ ,  $\Xi^-$ ,  $\Xi^0$ ) but considers Yukawa-type interaction terms only involving the  $\omega$  and the  $\rho$  meson fields. Additionally, our approach includes non-Yukawa many-

body interaction terms through nonlinear self-couplings involving the scalar-isoscalar  $\sigma$  meson. For more complete description see Ref. (Vasconcellos et al. 2014).

In our approach, the self-interaction terms are simulated by means of a parametrization of the coupling constants of the theory. For certain values of the parameters, the treatment adopted in this work reproduces the same predictions for global properties of neutron stars as most of the models based on Yukawa-type couplings involving the  $\sigma$ ,  $\omega$  and  $\rho$  mesons. For other choices of the parameters, our approach allows the description of the effects of density self-correlations of higher orders involving the scalar-isoscalar meson  $\sigma$  on global properties of neutron stars.

In the mean field approximation, the parameterized coupling Lagrangian density with scalar self-energy insertions,  $\Sigma_{B\lambda 0}^{s*}$ , is defined as (Vasconcellos 2012)

$$\begin{aligned} \mathcal{L}_\lambda = & \frac{1}{2}m_\sigma^2\sigma_0^2 + \frac{1}{2}m_\omega^2\omega_0^2 + \frac{1}{2}m_\rho^2\rho_{03}^2 \\ & + \sum_l \bar{\psi}_l (i\gamma_\mu\partial^\mu + q_e\gamma_\mu A^\mu - m_l) \psi_l \\ & + \sum_B \bar{\psi}_B (i\gamma_\mu\partial^\mu + q_e\gamma_\mu A^\mu - g_\omega B\gamma^0\omega_0) \psi_B \\ & - \sum_B \bar{\psi}_B \left( \frac{1}{2}g_{\rho B}\gamma^0\tau^{(3)}\rho_{03} + M_{B\lambda}\Sigma_{B\lambda 0}^{s*} \right) \psi_B, \end{aligned} \quad (3)$$

where the subscripts  $B$  and  $l$  represent, respectively, the baryon octet ( $n$ ,  $p$ ,  $\Lambda^0$ ,  $\Sigma^-$ ,  $\Sigma^0$ ,  $\Sigma^+$ ,  $\Xi^-$ ,  $\Xi^0$ ) and lepton ( $e^-$ ,  $\mu^-$ ) species. The electromagnetic interaction is introduced by the  $A^\mu$  field, with the coupling intensity given by the particles electrical charge  $q_e$ . In this expression,  $g_\Phi$ , with  $\Phi = \sigma, \omega, \rho$ , represents the effective baryon-meson coupling constants and  $\sigma_0$ ,  $\omega_0$  and  $\rho_{03}$  are the mean field values of the  $\sigma$ ,  $\omega$  and  $\rho_\mu$  meson fields. The self-energy insertion  $\Sigma_{B\lambda 0}^{s*}$  is defined as

$$\Sigma_{B\lambda 0}^{s*} = m_{B\lambda}^* \equiv \left( 1 + \frac{g_{\sigma B}\sigma_0}{\lambda M_B} \right)^{-\lambda}, \quad (4)$$

and gives rise to the effective parameterized baryon mass

$$\begin{aligned} M_{B\lambda}^* &= M_B m_{B\lambda}^* \\ &\simeq M_B \left( 1 - \frac{g_{\sigma B}\sigma_0}{M_B} + \left( \frac{\lambda}{2} \right) \left( \frac{g_{\sigma B}\sigma_0}{\lambda M_B} \right)^2 \right) + \mathcal{O}(3), \end{aligned} \quad (5)$$

for  $\frac{g_{\sigma B}\sigma_0}{\lambda M_B} \ll 1$ ; in this expression  $\left( \frac{\lambda}{2} \right)$  represents the generalized binomial coefficients of the expansion; we also emphasize in this expression the direct dependence of the effective baryon mass on the  $\lambda$  parameter of the model. Finally, note that our method is equivalent to replace the original Yukawa scalar coupling  $g_{\sigma B}\sigma$  by the parameterized scalar coupling

$$g_{\sigma B}\sigma \rightarrow g_{\sigma B\lambda}^*\sigma_0 \equiv m_{B\lambda}^*g_{\sigma B}\sigma_0. \quad (6)$$

Properties of the fields considered in our formulation are presented in table (1).

**Table 1** Properties of the fields considered in the formulation. In what follows, we use the abbreviations: ISS: isoscalar-scalar; ISV: isoscalar-vector; IVV: isovector-vector.

Fields	Classification	Particles	Coupling Constants	Mass (MeV)
$\psi_B$	Baryons	N, $\Lambda$ , $\Sigma$ , $\Xi$	N/A	939, 1116, 1193, 1318
$\psi_l$	Leptons	$e^-$ , $\mu^-$	N/A	0,5, 106
$\sigma$	ISS-meson	$\sigma$	$g_{\sigma B}^*$	550
$\omega_\mu$	ISV-meson	$\omega$	$g_{\omega B}^*$	782
$\varrho_\mu$	IVV-meson	$\rho$	$g_{\varrho B}^*$	770

In a previous contribution to this volume (Vasconcellos et al. 2014), we have determined the equation of state, population profiles and the mass-radius relation for families of neutron stars with hyperon content. In this contribution, we additionally consider the effects of strong magnetic fields on the properties of neutron stars with hyperon degrees of freedom.

### 3 Coupling constants

When constraining the coupling constants of our approach, we use the conventional procedure, which considers that the predictions of an effective theory must be in line with two-body scattering results and bulk static properties data of nuclear matter at saturation density. This means that the theory should reproduce the main properties of finite nuclei. After this, the next step comprises extrapolating the theory to the high density regime.

We constrain in the following the  $\lambda$  parameter in order to describe the effective mass of the nucleon and compression modulus at saturation density. We emphasize that our model predicts the values of nuclear saturation properties in good agreement with literature (shown in Table (2)). We have adopted for the saturation density of nuclear matter  $\rho_0 = 0.17 \text{ fm}^{-3}$  and for the binding energy  $\epsilon_B = -16.0 \text{ MeV}$ . The  $\lambda$  parameter is constrained to describe the nucleon effective mass at saturation between  $[0.70 - 0.78] \text{ MeV}$ . The isovector coupling constant  $g_{\varrho N}$  on the other hand was chosen to describe the symmetry energy coefficient  $a_{\text{sym}} = 32.5 \text{ MeV}$  (for more details see Haensel, Potekhin & Yakovlev 2007). Based on this, we introduce a coherent set of nuclear-meson coupling constants  $g_{\sigma N}$ ,  $g_{\omega N}$  for symmetric matter in the saturation density range.

In the high density regime, as already mentioned, hyperon degrees of freedom must be taken into account. However, since these fields are not present in nuclear matter at saturation density, it is not possible to determine the hyperon-meson (HM) couplings directly. In most models found in the literature, hyperon degrees of freedom appear in nuclear matter at around two times the nuclear saturation density  $\rho_0$ , as for instance, in relativistic mean-

field models (Wang et al. 2006), in non-relativistic potential models (Dabrowski & Rozynek 2010), in the quark-meson coupling model (Whittenbury et al. 2013), in relativistic Hartree-Fock models (Huber et al. 1998), in Brueckner-Hartree-Fock calculations (Shternin, Baldo & Haensel 2013), and within chiral effective Lagrangian (Banik et al. 2004). Nevertheless, the details of the hyperon composition of neutron star matter are rather sensitive to the chosen hyperon potentials.

**Table 2** Coupling parameters of our approach.

$\lambda$	$(\frac{M^*}{M})_0$	$K_0 \text{ (MeV)}$	$(\frac{g_{\sigma B}}{m_\sigma})^2$	$(\frac{g_{\omega B}}{m_\omega})^2$	$(\frac{g_{\varrho B}}{m_\varrho})^2$
0.06	0.70	262	11.87	6.49	3.69
0.10	0.75	226	10.42	5.10	3.94
0.14	0.78	216	9.51	4.32	4.07

As the density of the system increases, it becomes more energetically favorable for the system to create hyperon species than increase the energy levels of the nucleon. In order to describe the hyperon couplings, we define the hyperon-meson couplings as  $g_{\eta B} = \chi_{\eta B} g_{\eta N}$  for  $\eta = \sigma, \omega, \varrho$ . In this work, in order to constrain the hyperon population, we use the three hyperon coupling models that follows:

- **HYS(1)** (Moszkowski 1974): it is based on the different nature of hyperons with respect to nucleons:

$$\chi_{\sigma B} = \chi_{\omega B} = \chi_{\varrho B} = \sqrt{2/3}; \quad (7)$$

- **HYS(2)** (Pal et al. 1999): it is based on the counting quark rule.

$$\chi_{\sigma \Lambda} = 2/3, \quad \chi_{\sigma \Sigma} = 2/3, \quad \chi_{\sigma \Xi} = 1/3, \quad (8)$$

$$\chi_{\omega \Lambda} = 2/3, \quad \chi_{\omega \Sigma} = 2/3, \quad \chi_{\omega \Xi} = 1/3, \quad (9)$$

$$\chi_{\varrho \Lambda} = 0, \quad \chi_{\varrho \Sigma} = 2, \quad \chi_{\varrho \Xi} = 1; \quad (10)$$

- **HYS(3)** (Rufa et al. 1990; Glendenning & Moszkowski 1991): it is based on experimental analysis of  $\Lambda$ -hypernucleus data

$$\chi_{\sigma B} = \chi_{\sigma \Lambda}; \quad \chi_{\omega B} = \chi_{\omega \Lambda}; \quad \chi_{\varrho B} = 0, \quad (11)$$

where the binding energy is given by:

$$\begin{aligned} (B/A)_\Lambda &= \chi_{\omega B} (g_{\omega N} \omega_0) + \chi_{\sigma B} (m_\Lambda^* - m_\Lambda) \\ &= -28 \text{ MeV}, \end{aligned} \quad (12)$$

and

$$\chi_{\sigma \Lambda} = 0.75. \quad (13)$$

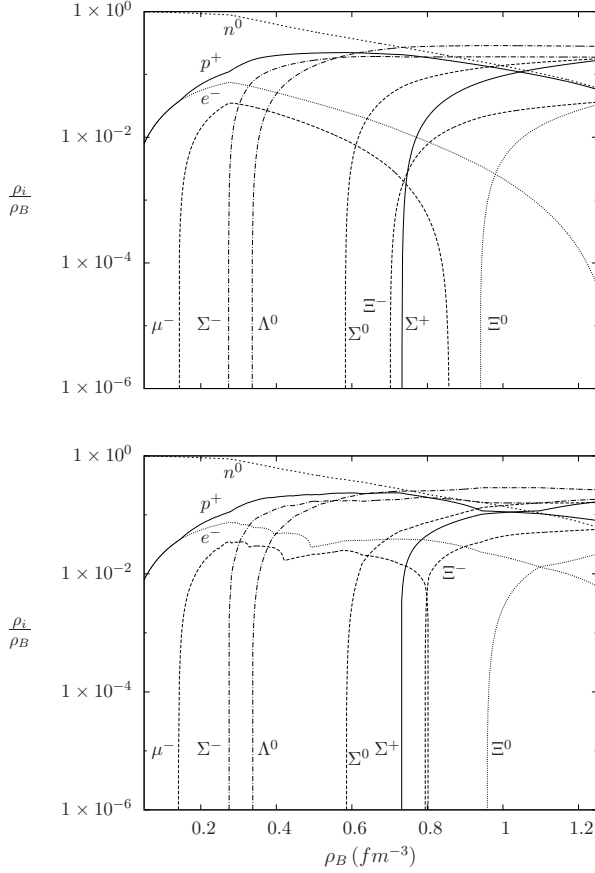


**Fig. 1** Particles densities (divided by baryon density) as a function of the baryon density, using the hyperon coupling model *HYS*(1) and the parametrization from table 2 ( $\lambda = 0.06$ ). The top panel does not have magnetic field contributions. The bottom panel includes magnetic field contributions, with  $B_c = 10^{19} \text{ G}$ .

#### 4 Magnetic field and Landau quantization

In the presence of an external magnetic field  $B$  in the  $z$  direction, the orbital motion of charged particles (baryons and leptons) is described by the Landau quantization energy spectra

$$E_{\nu,i} = \sqrt{k_{z,i}^2 + m_i^2 + 2\nu|q_e|B}, \quad (14)$$

with  $i = B, l$ . Note that in the expression above we must consider the effective mass of baryons. The Landau levels are double degenerated except for the fundamental state, and are enumerated by  $\nu$ . We calculate the EoS from the spatial and temporal contributions of the energy-momentum tensor of the system, following the solutions already calculated in the literature by (Broderick, Prakash & Lattimer 2002).

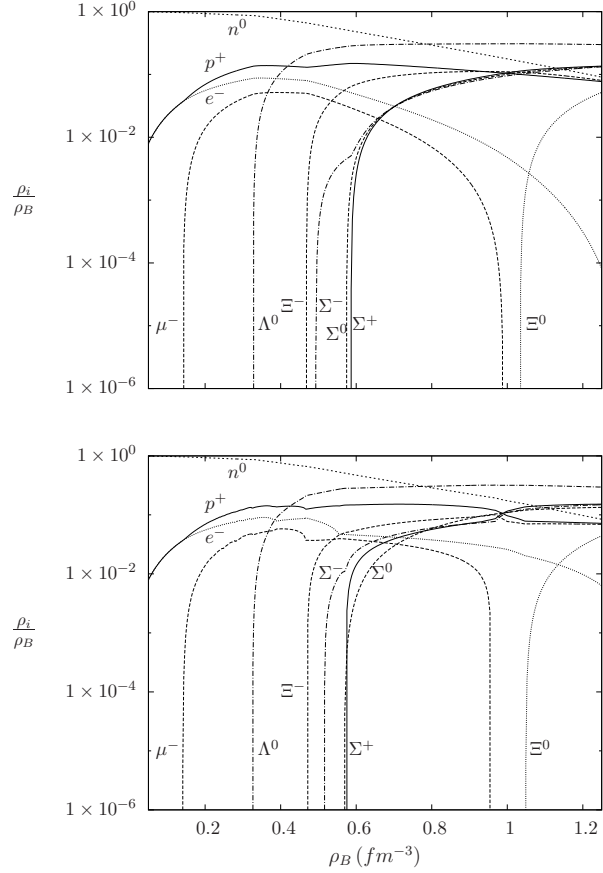


**Fig. 2** Same as figure 1, but for the hyperon coupling model *HYS*(2).

The equation of state  $P_{mag} = P_{mag}(\varepsilon_{mag})$  may be expressed as

$$\begin{aligned} \varepsilon_{mag} = & \frac{1}{2}m_\sigma^2\sigma_0^2 + \frac{1}{2}m_\omega^2\omega_0^2 + \frac{1}{2}m_\rho^2\rho_0^2 \\ & + \frac{|q_e|B}{4\pi^2} \sum_{b,\nu} \eta(\nu) \left[ k_{F_{b,\nu}} \mu_b^* + \bar{m}_{b,\nu}^2 \ln \left( \frac{\mu_b^* + k_{F_{b,\nu}}}{\bar{m}_{b,\nu}} \right) \right] \\ & + \frac{|q_e|B}{4\pi^2} \sum_{l,\nu} \eta(\nu) \left[ k_{F_{l,\nu}} \mu_l + \bar{m}_{l,\nu}^2 \ln \left( \frac{\mu_l + k_{F_{l,\nu}}}{\bar{m}_{l,\nu}} \right) \right], \end{aligned} \quad (15)$$

with

$$\begin{aligned} P_{mag} = & -\frac{1}{2}m_\sigma^2\sigma_0^2 + \frac{1}{2}m_\omega^2\omega_0^2 + \frac{1}{2}m_\rho^2\rho_0^2 \\ & + \frac{|q_e|B}{4\pi^2} \sum_{b,\nu} \eta(\nu) \left[ k_{F_{b,\nu}} \mu_b^* - \bar{m}_{b,\nu}^2 \ln \left( \frac{\mu_b^* + k_{F_{b,\nu}}}{\bar{m}_{b,\nu}} \right) \right] \\ & + \frac{|q_e|B}{4\pi^2} \sum_{l,\nu} \eta(\nu) \left[ k_{F_{l,\nu}} \mu_l - \bar{m}_{l,\nu}^2 \ln \left( \frac{\mu_l + k_{F_{l,\nu}}}{\bar{m}_{l,\nu}} \right) \right]. \end{aligned} \quad (16)$$

We also allow the pressure to become anisotropic in the presence of a strong magnetic field, as pointed out by Refs. (Perez Martinez, Perez Rojas & Mosquera Cuesta 2008; Strickland, Dexheimer & Menezes, 2012; Paulucci et al

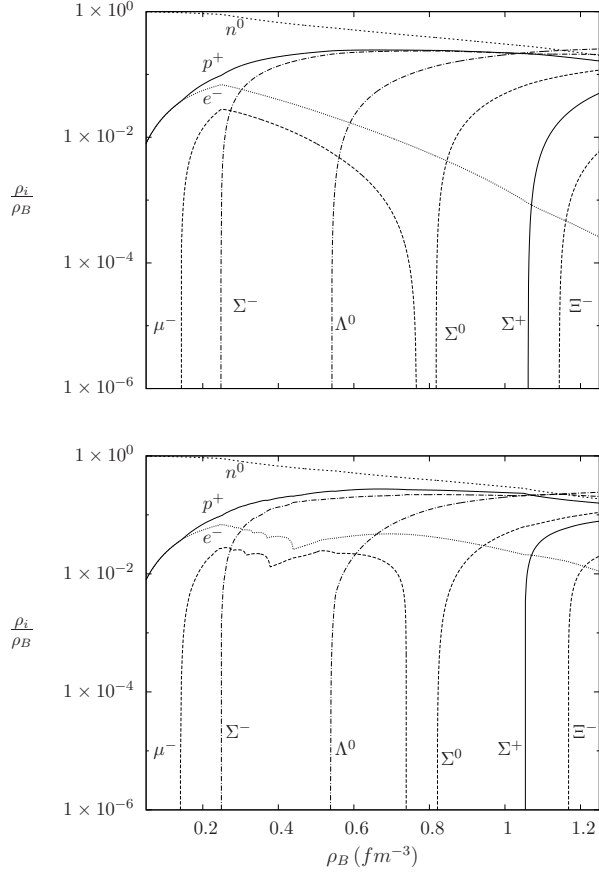


**Fig. 3** Same as figure 1, but for the hyperon coupling model HYS(3).

2011)

$$\varepsilon = \sum_{B,l} \varepsilon_{mag} + \frac{B^2}{2}; P_{\parallel} = \sum_{b,l} P_{mag} - \frac{B^2}{2},$$

$$P_{\perp} = \sum_{b,l} P_{mag} + \frac{B^2}{2} - B\mathcal{M}, \quad (17)$$

where the magnetization is calculated as  $\mathcal{M} = \partial P_{mag} / \partial B$ .

We assume a magnetic field with chemical potential dependence (Bandyopadhyay et al. 1997; Dexheimer et al. 2012):

$$B(\mu) = B_{surf} + B_c [1 - \exp(-b(\mu_n - 938)^a)], \quad (18)$$

where  $B_c$  represents the magnetic field in the high  $\mu_n$  limit and the parameters  $a$  and  $b$  determine how fast the magnetic field increases towards the center of the star.

## 5 Results and conclusions

We model particle populations considering the conditions of beta-equilibrium, charge neutrality and baryon number conservation. Also, we assume that the baryon chemical potential suffers a shift by the vector mesons due to the nuclear interaction:

$$\mu_i^* = q_{b_i} \mu_n - q_{e_i} \mu_e - g_{\omega} \omega - g_{\varrho} \frac{\tau}{2}. \quad (19)$$

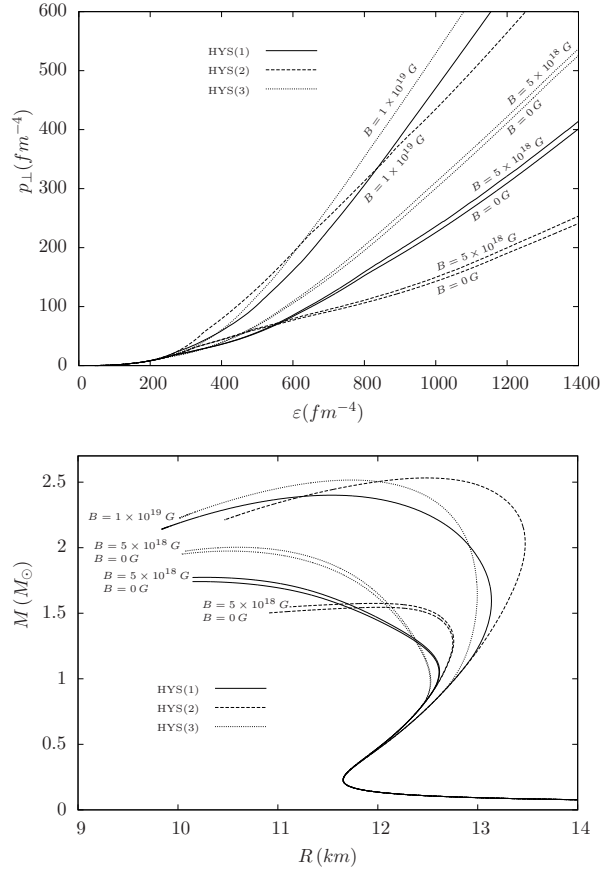


**Fig. 4** EoS (top panel) and mass-radius diagram (bottom panel) for different central magnetic fields  $B_c$ , and different hyperon coupling model. All curves use the first parametrization on table 2 ( $\lambda = 0.06$ ).

In addition, our hadronic model considers magnetic effects on the hyperon population of neutron stars with strong magnetic fields. As can be seen in the top panel of Figs. (1), (2) and (3), the different hyperon coupling models reproduce quite different star populations.

The chemical potential of particles is responsible for their appearance in the system and it is calculated based on the coupling constants with the mesons. More precisely, the coupling with vector mesons lowers the chemical potential, allowing the baryons to be created at lower densities, among other conditions. In particular, the HYS(3) proposes that all hyperon species have a zero coupling constant with the meson  $\varrho$ , implying a higher chemical potential. The consequence of this choice of model is the appearance of hyperon species only at high densities - in comparison with HYS(1) and HYS(2) - which have the direct effect of stiffening the EoS, as shown in the top panel of Fig. (4).

Moreover, the introduction of magnetic fields in the model raises several new issues concerning the star population which are discussed in the following. The first one is the change in the order that the hyperons appear as a function of density, like for example the  $\Sigma^+$  and  $\Xi^-$  in the bottom panel

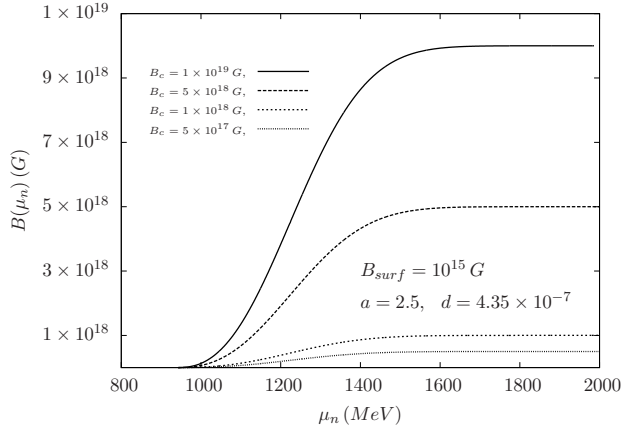


**Fig. 5** Magnetic field dependence on baryon chemical potential. We use the parameterization:  $a = 2.5$ ,  $b = 4.35 \times 10^{-7}$ , and a surface magnetic field of  $B_{surf} = 10^{15} \text{ G}$ , the highest one measured (Dexheimer 2011).

of Fig. (1). The second one is the change in the amount of charged particle species, like for example the electrons at high densities in the bottom panel of Fig. (3). The third issue is the wiggles that appear due to the Landau quantization and integer values of  $\nu$ , which can be clearly seen for example in the bottom panel of Fig. (2). These would be even more different (from the case in which the magnetic field was ignored) if we had included the effects of anomalous magnetic moment in the model, as done in Refs. (Dexheimer, Negreiros & Schramm 2012; Isayev & Yang 2013). In such case, the population of particles with different spins becomes quite different, and in some cases, fully polarized.

The difference in particle population caused by the magnetic field also affects the EoS, as seen in the top panel of Fig. (4). Besides the effect of clearly stiffening all EoS at high densities, the magnetic field exchanges the order (according to stiffness) of the EoS of different hyperon coupling models at intermediate densities. For example, the curve for the HYS(2) with  $B_c = 10^{19} \text{ G}$  at  $\epsilon \sim 600 \text{ fm}^{-4}$ , which was the softer EOS without magnetic field but becomes the stiffer one in the presence of strong magnetic field. This in turn, makes the HYS(2)-EoS to reproduce more massive stars (compared with the other hyperon coupling models) but only in the presence of strong magnetic fields. This can be seen in the bottom panel of Fig. (4).

All these effects are up to some extent model dependent. Nevertheless, they still contain relevant physical conclusions, such as the importance of better understanding the magnetic field dependence with density and on the structure of neutron stars. The dependence of the EoS and particles population on the different hyperon-meson couplings models at high densities also highlights the fact that a better analysis of the hyperon-meson coupling needs to be explored in order to quantify the effect of these uncertainties on the observable properties of neutron stars.

## References

- Bandyopadhyay, D., Chakrabarty, S., Pal, S.: 1997, Phys. Rev. Lett. 79, 2176
- Belvedere R., Pugliese D., Rueda J. A., Ruffini R., Xue S.-S.: 2012, Nucl. Phys. A 883, 1
- Bethe, H. A., Brown, G.: 1998, ApJ 506, 780
- Broderick, A., Prakash, M., Lattimer, J.: 2002, Phys.Lett. B531, 167
- Buballa, M., Dexheimer, V., Drago, A., Fraga, E., Haensel, P., Mishustin, I., Pagliara, G., Schaffner-Bielich, J., Schramm, S., Sedrakian, A., Weber, F.: 2014, arXiv:1402.6911v1 [astro-ph.HE]
- Demorest, P., Pennucci, T., Ransom, S., Roberts, M., Hessels, J.: 2010, Nature 467, 1081
- Dexheimer, V., Vasconcellos, C.A.Z., Bodmann, B.: 2008, Phys.Rev. C 77, 065803
- Dexheimer, V., Negreiros, R., Schramm, S.: 2012, Eur. Phys. J. A48, 189; 2013, J. Phys. Conf. Ser. 432, 012005
- Ferrer, E.J., de la Incera, V., Keith, J.P., Portillo, I., Springsteen, P.L.: 2010, Phys. Rev. C82, 065802
- Glendenning, N., Moszkowski, S.: 1991, Phys. Rev. Lett. 67, 2414
- Isayev, A., Yang J.: 2013 J.Phys. G40 035105 (Preprint 1210.3322)
- Malheiro, M., Rueda J. A., Ruffini R.: 2012, PASJ 64, 56
- Mereghetti, S.: 2008, Astron. Astropys. Rev. 15, 225
- Moszkowski, S.A.: 1974, Phys. Rev. D9, 1613
- Pal, S., Hanauske, M., Zakout, I., Stoecker, H., Greiner, W.: 1999, Phys. Rev. C60, 015802
- Paulucci, L., Ferrer, E.J., de La Incera, V., Horvath, J.E.: 2011, Physical Review D 83 (4), 043009
- Perez-Martinez, A., Perez-Rojas, H., Mosquera-Cuesta, H.: 2008, Int. J. Mod. Phys. D17, 2107
- Oppenheimer, J., Volkoff, G.: 1939, Phys. Rev. 55, 374
- Rufa, M., Schaffner, J., Maruhn, J., Stoecker, H., Greiner, W.: 1990, Phys.Rev.C42, 2469
- Strickland, M., Dexheimer, V., Menezes, D.: 2012, Phys. Rev. D86, 125032
- Taurines, A., Vasconcellos, C.A.Z., Malheiro, M., Chiapparini, M.: 2001, Phys. Rev. C63, 065801
- Tolman, R.C.: 1939, Phys. Rev. 55, 364
- Woods, P.M., and Thompson, C., 2006 ; in Compact Stellar X-ray Sources, ed. W. H. G. Lewin and M. van der Klis (UK: Cambridge University Press).